Vortices and field correlations in the near-field speckle of a three dimensional photonic crystal

Silvia Vignolini,[1,*] Matteo Burresi,[2] Stefano Gottardo,[1] L. Kuipers,[2] and Diederik S. Wiersma[1]

[1] *European Laboratory for Non-linear Spectroscopy (LENS) and INFM-BEC, Via N. Carrara, 1. I-50019 Sesto Fiorentino Firenze, Italy*

[2] *FOM Institute for Atomic and Molecular Physics (AMOLF) Kruislaan 407 Amsterdam N-41883 1009 DB Amsterdam, The Netherlands*

We present an experimental study of near-field speckle observed from photonic crystals and analyze this speckle from different perspectives. We observed vortices in these speckle patterns and analyze their statistical properties and morphological parameters. This allows to make a comparison between speckle from photonic crystals and that from completely random systems. Analysis of the field correlation functions allows to determine important sample parameters like the transport mean free path, diffusion constant, and effective refractive index.

Photonic crystals, no matter how accurately prepared, contain a certain level of disorder due to size fluctuations of the scattering elements and other structural imperfections. This disorder can be small but it usually plays an important role in determining their optical properties, especially in the case of three dimensional photonic crystals [1]. Disorder does not destroy interference, but it makes the optical behavior of photonic crystals much more complex and it gives rise to multiple scattering which leads to intensity patterns, known as speckle [2]. The phase and amplitude distributions of a speckle pattern contain important information like the local density of states [3], and exhibit interesting features like phase singularities [4–7]. Even if the understanding of speckle patterns in terms of amplitude and phase for disordered systems is rapidly growing [8–12], little is know about their behavior in partially ordered systems like photonic crystals. In pioneering theoretical work on this topic, it was shown that the speckle generated by the intrinsic disorder in a photonic crystal contains a lot of useful information, in a particular on the strength of the photonic bandgap [13]. No experiments have been reported up to today on speckle from photonic crystals.

Here we report on the experimental study and analysis of speckle patterns generated by three dimensional photonic crystals with a certain degree of disorder. We have performed this study in the near-field using a phase sensitive technique, to maximize the amount of information that one can obtain. We observe and analyze different properties of the speckle patterns that are known to exist in random systems but have not been observed in periodic structures so far. We find, for instance, that these speckle patterns contain phase singularities (vortices), and we have characterized their morphological and statistical parameters. We highlight both the aspects that are and are not in agreement with the far-field theory of phase vortices for random system. The complete characterization of the electric field in terms of amplitude and phase enabled us to analyze the spatial and the spectral correlation function of the field, which can be used to determine sample parameters like the average refractive index, mean free path, and diffusion constant of photonic crystals.

The sample under investigation is a silica synthetic opal grown using a dip coating technique [14]. The microspheres that constitute the photonic structure have a diameter of 730nm. A Scanning Electron Microscope (SEM) image of the sample is provided in the inset (I) of Figure 1(a). Reflection measurements, performed along the Γ direction of the opal, exhibit a Bragg peak centered at 1550nm with a reflectivity of roughly 30%. See inset (II) in Figure 1(a). This low value of reflectivity indicates that the opal has an appreciable degree of disorder. We have performed a set of measurements in the same zone of the sample for different incident wavelengths ranging from 1440nm to 1590nm using a Scanning near-field Microscope (SNOM) combined with a Mach-Zehnder type interferometer. This technique has been shown to be very efficient in analyzing the optical properties of photonic materials and in particular photonic crystals [15–17]. Figure 1(b) provides a schematic description of the setup. Linearly polarized laser light along the x direction is coupled into the structure by focussing it at one side of the [111] plane of the opal. An aluminum-coated tapered fiber with a sub-wavelength aperture (near-field probe) [18] is kept at $\sim$ 20nm of distance from the sample. A minute fraction of the evanescent field of the light propagating through the sample is coupled to the probe and detected. Combining a near-field microscope with a interferometer provides amplitude and phase information of the light for every position of the probe. In this way both the amplitude and the phase distributions are achievable with sub-wavelength resolution [19, 20] allowing us to reconstruct the field as:

$$F(x,y) = A(x,y)\exp i\varphi(x,y) = f_{Re}(x,y) + i f_{Im}(x,y), \quad (1)$$

where A and φ indicate the amplitude and the phase of the optical field, and f_{Re} and f_{Im} its Real and Imaginary parts, respectively.

Figure 1(c) shows a typical map of the electric field

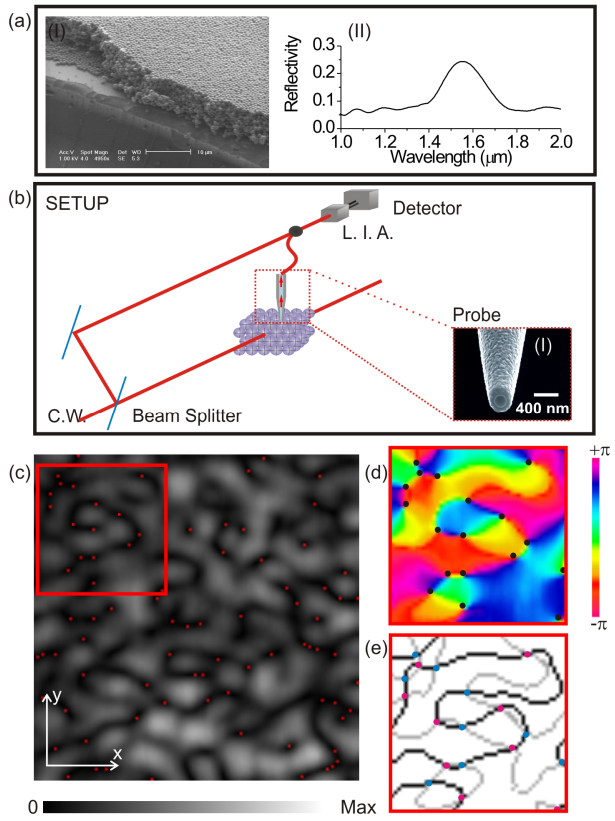

FIG. 1: (a) (I) Scanning Electron Microscope image of at the edge of the opal. (II) Reflection measurement along the Γ direction. (b) Schematic representation of the experimental setup. A tunable laser light source is coupled into the three-dimensional photonic crystal. The probe of the microscope (a scanning electron microscope image is provided in the inset) collects a fraction of the field inside the sample. This light is interferometrically mixed with the reference light of the same laser. Only the resulting interference signal is recorded. (c) Example of the the electric field amplitude distribution collected by the near-field microscope at $\lambda = 1442$nm. The red dots in correspondence of the zero values of the field amplitude correspond to the position of vortices. The dimension of the red box is 4 by 4μm. (d) and (e) are two zooms in the zone indicated by the red square. In particular, (d) is the map of the phase as a function of position, (e) is the map of the zero lines of the real part and the imaginary part of the field. The intersections of these two lines, indicated with the colored circles, represent the position of vortices.

amplitude collected by the near-field probe where the speckle fluctuations characteristic of random systems are clearly recognizable. Figure 1(d) provides the map of the phase collected in the red square. Focusing our attention on this image, we can easily recognize the phase singularities. To locate the vortex position accurately in the maps we identify the lines where both f_{Re} and f_{Im} are zero. The vortex centers are located at the crossing points of these lines. In Figure 1(e), the zero crossing map of f_{Re} (grey line) and f_{Im} (black line) is provided. Now the vortex positions are indicated by the colored circles at the intersections between these lines. Freund *et al.* showed that these vortices must obey a fundamental sign-principle, namely that nearest neighbors on the same zero crossing line should be of opposite sign [6]. This means that, when a certain vortex has an increasing phase when rotating clockwise, its adjacent on a zero crossing should have a decreasing phase when rotating in the same direction. The reason behind this concept is topological, and should therefore hold for any type of vortex field, including that one generated by a partially disordered photonic crystal. To verify the sign principle, we calculated along the two directions in the plane, the derivatives of the phase at the position of the vortices. This method provides a simple way of determining whether the phase increases or decrease when rotating around the phase singularity. We find that nearest neighbors are indeed anti-correlated. As much as 85% of the identified vortices have nearest neighbors of opposite sign. The fact that we do not find an anti-correlation of 100% can be attributed to errors in the identification of vortices itself, due to the finite spatial resolution. To provide a more detailed characterization of the vortex field, we calculated from the experimental data the vortex morphological parameters and their statistical probability densities. We compare our experimental results with the theoretical results for fully disordered structures [21, 22]. It is convenient to investigate the statistical behavior of the geometrical parameters associated to the tangent planes of f_{Re} and f_{Im} at the vortex position. In particular, we define ρ_{Re} and ρ_{Im} as the angles between the normal of the tangent planes and the x axis, and with $\tan\phi_{Re}$ and $\tan\phi_{Im}$ their slopes. Figure 2(a) provides a schematic representation of these parameters. In Figure 2(b) the angular distribution ρ_{Re} is presented. This distribution shows two well-defined maxima in correspondence of $\pm\frac{\pi}{2}$. For the angular distribution of ρ_{Im}, which is not reported here, the same behavior is obtained. The fact that the vortices are predominantly orientated along the y axis (that is, perpendicular with respect the polarization direction) can be attributed to the polarization dependence of the speckle pattern in the near-field [23–26]. Figure 2(c) shows the probability distribution of the vortex amplitude $a = \tan\phi_{Re}$. This probability is analogous to the one calculate for the isotropic random case. Finally in Figure 2(d) the probability distribution of the vortex anisotropy ($\alpha = \frac{\tan\phi_{Im}}{\tan\phi_{Re}}$) is reported. The obtained values for α are extremely small and consequently in the histogram the bin that contains most counts is the one that also contains $\alpha = 0$, indicating that in most cases the vortices present a substantial degree of anisotropy. The same statistical behavior of these parameters is observed for the entire wavelength range that we have investigated in the experiments. To improve the signal to noise ratio of the analysis, the prob-

ability distributions reported in Figure 2 are therefore averaged over all wavelengths. In addition to the mor-

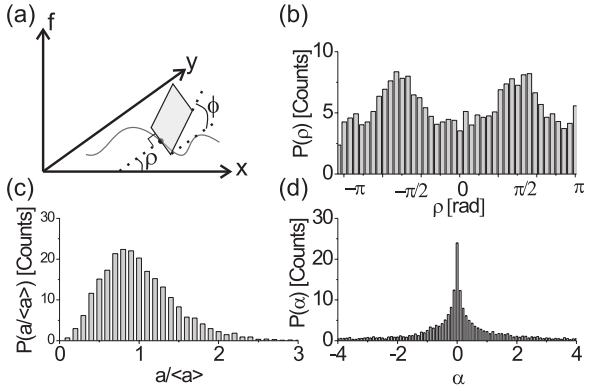

FIG. 2: (a) Schematic representation of the geometry of the real imaginary tangent plane: the angle that measure the orientation of the plane respect to the x axes is ρ, while the slope of the plane is ϕ. (b)-(d) Vortex morphological parameters distributions for ρ, a and α , respectively.

phological proprieties of the vortices, it is important to consider their spatial distribution as well [27]. First of all we observe that their density is comparable, within the error, with the half of the inverse of the coherence area as expected for the far-field case. Figure 3(a) presents the histogram of the distance distribution between vortex centers for the first, second and third neighbors. In order to highlight effects of spatial correlation, we compare these distances with the case of a completely random distribution. After defining $\beta = d_m/d_r$ as the ratio of the measured average n-th nearest neighbor separation(d_m) to that calculated for the random distribution (d_r), we notice that the vortices are systematically spaced more widely apart than would be expected for a purely random distribution. Figure 2(b) shows the values of β for the first seven neighbors, which reveals that the vortices appear to weakly repel one to another, as expected theoretically [6].

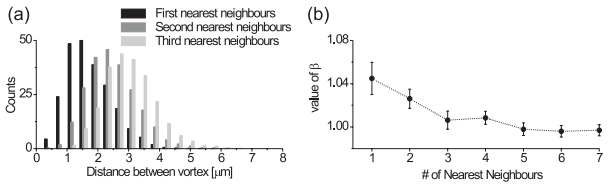

FIG. 3: (a) Histogram of the distances distribution between vortex centers for the first, second and third neighbors. (b) Value of β for first to seventh nearest neighbors, in the inset the total number of vortex is reported as the wavelength is varied.

A polarization dependencies of the speckle pattern it is present in the spatial correlation of the electric field, defined as $C_E(\Delta x, \nu) = < E(x,\nu)E^*(x+\Delta x,\nu) >$. This quantity yields information about the transport proprieties of the sample that are usually hidden inside the speckle pattern. Figure 4(a) shows the spatial correlation function obtained from the measurements, at $\lambda = 1442$nm. In the figure we observe an evident radial anisotropy. In particular we can recognize principally two aspects: first, the spatial correlation length of the field is much larger in the direction of the polarization (x) than in the perpendicular direction. Second, there are other anisotropic features that depends on the selected direction and on the wavelength. The first type of anisotropy of the correlation function is independent from the wavelength and so we exclude that it is induced by the photonic structure. While in the second case, the other anisotropic features in the image are wavelength dependent and indicate an underlying spatial periodic structure. In fact, for a complete random sample they are expected to vanish exponentially with the distance from the center. Since a complete theory that describes the near-field speckle pattern of an ordered medium with an appreciable degree of disorder is still missing, we compare our results with the ones obtained for a fully random structure. This comparison can still give some insight by looking at the similarities and differences. The fact that the correlation length is larger along the polarization direction respect to the perpendicular direction is well explained considering that speckle pattern in the near-filed is polarization dependent [25, 26]. Moreover, we find that the experimental spatial correlation profile along the y axis matches very well the theoretical curve for random systems, given by Freund *et al.* in [28]. See Fig.4(b). This allows us to perform a fit to the value of the effective refractive index which gives the value: $\mathbf{n} = 1.07 \pm 0.07$. This value is constant within the error for all the wavelengths considered and it is in agreement with Maxwell-Garnett theory.

The profile along the x axis, on the other hand, does not have the same shape and it is not possible to find a match with the same theory. Figure 4(b) also provides the profile along the y axes of the imaginary part of the spatial correlation function. This imaginary part should vanish in a homogeneous isotropic system, as can be easily seen as follows. In this case we have $C_E(\Delta x) = C_E(-\Delta x)$, due to translational invariance, so that $C_E(\Delta x) = C_E^*(-\Delta x)$. In our case we can clearly see that the imaginary part is not zero but exhibits oscillations. These oscillations are most likely due to the underlying photonic crystal structure, which is spatially periodic. By calculating the spectral correlation function $C_E(\Delta\nu) =< E(\nu)E^*(\nu+\Delta\nu) >$, it is in principle possible to determine the diffusion constant and mean free path of a system. The brackets denote an ensemble average. We have calculated this correlation function for our data, taking the average over different (distant) positions on the sample. Figure 4(c) provides the spectral correlation function obtained this way from the measurements,

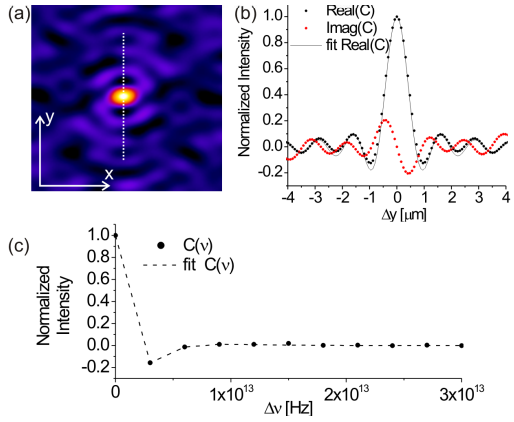

FIG. 4: (a) Real part of the spatial correlation function of the electric field. (b) The dotted black line reports the cut along the y direction of the real part of the correlation function, while the gray dotted line represent the imaginary part of the correlation function. The black straight line is the fit of the real part of the correlation function obtained considering the theory for random systems reported in [11]. The dotted line in panel (a) (dimension of total scan is 8 by 8μm) represents the position where the dotted black cut in figure (b) is taken. (c) The dashed black line is the theoretical spectral field correlation (as presented in [11]) while the dots represent the experimental data.

compared with theory for random systems [11]. We find a good agreement between the two curves if we consider a mean free path of $l = 2.2 \pm 0.5\mu$m and a diffusion constant of $D = 70 \pm 10\text{m}^2/\text{s}$ fixing for the refractive index the value $n = 1.07$ obtained from the spatial correlation function, and considering the minimum sample dimension of $L = 12 \pm 2\mu$m. From the comparison we also can estimate that the absorbtion length in the sample, which is found to be of the order of 10^3 mm.

In conclusion we have studied the phase and amplitude of speckle generated by photonic crystals, in the near-field regime. We observe vortices and by studying the statistical properties of their morphological parameter find analogies and differences with respect to random systems. In addition, we measured and analyzed the field correlations of the near-field speckle and estimated from that the amount of disorder in the system. In order to develop a complete theory that can take into account both the effects of random multiple scattering and the underlying photonic crystal order one would have to calculate the Green's function for propagation taking into account both effects. Ideally this calculation should include also the polarization, since this is expected to by very important in a photonic crystal based structure.

We wish to thank Boris Shapiro, Francesca Intonti and Riccardo Sapienza for fruitful discussions. This work was made possible by the characterization facilities of the Amsterdam nanoCenter. It is part of the research program of the "Stichting voor Fundamenteel Onderzoek der Materie (FOM)", financially supported by the "Nederlandse Organisatie voor Wetenschappelijk Onderzoek (NWO)".This work was also financially supported by the European Network of Excellence on nanophotonics Phoremost. (IST-2-511616-NoE)

* vignolini@lens.unifi.it

[1] See e.g. A. F. Koenderink, A. Lagendijk, and W. L. Vos, Phys. Rev. B. **72**, 153102 (2005).
[2] J. W. Goodman, *Statistical Optics* (John Wiley, New York, 1985).
[3] A. Z. Genack, P. Sebbah, M. Stoytchev, and B. A. van Tiggelen, Phys. Rev. Lett. **82**, 715 (1999).
[4] J. F. Nye and M. V. Berry, Proc. R. Soc. Lond. A **336**, 165 (1974).
[5] W. Wang, S. G. Hanson, Y. Miyamoto and M. Takeda, Phys. Rev. Lett. **94**, 103902 (2005).
[6] N. Shvartsman and I. Freund, Phys. Rev. Lett. **72**, 1008 (1994).
[7] S. Zhang A. Z. Genack, Phys. Rev. Lett. **99**, 203901 (2007).
[8] B. Shapiro, Phys. Rev. Lett. **57**, 2168 (1986).
[9] A. Z. Genack, Phys. Rev. Lett. **58**, 2043 (1987).
[10] J. H. Li, and A. Z. Genack, Phys. Rev. E **49**, 4530 (1994).
[11] P. Sebbah, R. Pnini, and A. Z. Genack, Phys. Rev. E **62**, 7348 (2000).
[12] P. Sebbah, B. Hu, A. Z. Genack, R. Pnini, and B. Shapiro, Phys. Rev. Lett. **88**, 123901 (2002).
[13] V. M. Apalkov, M. E. Raikh, and B. Shapiro, Phys. Rev. Lett. **92**, 253902 (2004).
[14] P. Jiang, J. F. Bertone, K. S. Hwang, and V. L. Colvin, Chem. Mater. **11**, 2132 (1999).
[15] E. Fluck, N. F. van Hulst, W. L. Vos, and L. Kuipers, Phys. Rev. E. **68**, 015601 (2003).
[16] K. Bittkau, R. Carius, A. Bielawny and R. B. Wehrspohn, J. Mater. Sci. Mater. Electron. pubblished on-line (2008).
[17] A. Nesci, R. Dndliker, M. Salt, and H. P. Herzig, Opt. Commun. **205**, 229 (2002).
[18] J. A. Veerman, A. M. Otter, L. Kuipers, and N. F. van Hulst Appl. Phys. Let. **72**, 3115 (1998).
[19] B. Deutsch, R. Hillenbrand, and L. Novotny, Opt. Express **16**, 494 (2008).
[20] M. L. M. Balistreri, , J. P. Korterik, L. Kuipers, and N. F. van Hulst, Phys. Rev. Lett. **85**, 294 (2000).
[21] I. Freund and N. Shvartsman, Phys. Rev. A **50**, 5164 (1994).
[22] I. Freund, J. Opt. Soc. Am. A **11**, 1644 (1994).
[23] V. Emiliani, F. Intonti, M. Cazayous, D. S. Wiersma, M. Colocci, F. Aliev and A. Lagendijk, Phys. Rev. Lett. **90**, 250801 (2003).
[24] J.-J. Greffet , R. Carminati, Ultramicroscopy **61**, 43 (1995).
[25] A. Apostol and A. Dorariu, Phys. Rev. Lett. **91**, 93901 (2003).
[26] C. Liu and S.-H. Park, Opt. Lett. **30**, 1602 (2005).
[27] N. Shvartsman and I. Freund, J. Opt. Soc. Am. A **10**, 2710 (1994).
[28] I. Freund and D. Eliyahu, Phys. Rev. A **45**, 6133 (1992).